Supplementary Information

For

Metal Coordination-Driven Photochromism in Schiff bases incorporating 1,2,4-triazole and hydroxyphenyl moieties

Aleksei A. Anisimov,*[a,b] Anna A. Bovkunova[a], Ekaterina V. Dubasova[a], Victoria E. Gontcharenko[b,c], Ilya V. Taydakov[b,c], Evgeniya S. Bazhina[a], Igor L. Eremenko[a] and Ivan V. Ananyev[a,b]

[a] N. S. Kurnakov Institute of General and Inorganic Chemistry, Russian Academy of Sciences, 31 Leninsky prosp., 119991 Moscow, Russian Federation, e-mail: anisimov.alex.a@gmail.com

[b] Faculty of Chemistry, National Research University Higher School of Economics, 20 Miasnitskaya Str., Moscow 101000, Russia

[c] P. N. Lebedev Physical Institute of the Russian Academy of Sciences, 53 Leninskiy. Pr-t, Moscow 119991, Russia

Table of Contents

XRD experimental data.

Table S1. Structural data and refinement parameters for **2**, **3**, **5**.

	2	**3**	**5**
Identification code	ab1122p1	ab1193	ab1198
Empirical formula	$C_{20}H_{20}Cl_2N_8O_4Zn$	$C_{22}H_{20}N_{10}O_4S_2Zn$	$C_{28}H_{20.4}N_{10}O_{2.2}S_2Zn$
Formula weight	572.71	617.97	661.63
Temperature/K	120.0	120.15	120
Crystal system	triclinic	monoclinic	triclinic
Space group	P-1	C2	P-1
a/Å	6.3811(6)	26.234(6)	9.2371(8)
b/Å	13.3652(13)	6.6881(17)	13.0112(12)
c/Å	15.4291(15)	7.4495(19)	14.2113(13)
α/°	114.694(5)	90	115.986(3)
β/°	90.702(5)	95.128(8)	93.532(3)
γ/°	101.967(5)	90	108.249(3)
Volume/Å^3	1162.3(2)	1301.8(6)	1418.0(2)
Z	2	2	2
ρ_{calc}g/cm^3	1.636	1.577	1.55
μ/mm^{-1}	1.333	1.155	1.062
F(000)	584.0	632.0	676
Crystal size/mm^3	0.08 × 0.03 × 0.03	0.164 × 0.15 × 0.01	0.08 × 0.04 × 0.02
Radiation	MoKα (λ = 0.71073)	MoKα (λ = 0.71073)	MoKα (λ = 0.71073)
2Θ range for data collection/°	2.924 to 56.65	5.49 to 56.534	3.278 to 55.996
Index ranges	$-8 \le h \le 7$, $-17 \le k \le 17$, $-20 \le l \le 20$	$-34 \le h \le 34$, $-8 \le k \le 7$, $-9 \le l \le 9$	$-12 \le h \le 12$, $-17 \le k \le 17$, $-18 \le l \le 18$
Reflections collected	11159	5371	29151
Independent reflections	5622 [R_{int} = 0.0425, R_{sigma} = 0.0748]	2936 [R_{int} = 0.0436, R_{sigma} = 0.1170]	6833 [R_{int} = 0.1003, R_{sigma} = 0.1092]
Data/restraints/parameters	5622/0/326	2936/1/191	6833/0/397
Goodness-of-fit on F^2	1.051	0.897	1.042
Final R indexes [I>=2σ (I)]	R_1 = 0.0569, wR_2 = 0.1452	R_1 = 0.0422, wR_2 = 0.0713	R_1 = 0.0536, wR_2 = 0.1200
Final R indexes [all data]	R_1 = 0.0859, wR_2 = 0.1558	R_1 = 0.0829, wR_2 = 0.0789	R_1 = 0.0944, wR_2 = 0.1361
Largest diff. peak/hole / e Å^{-3}	0.99/-0.98	0.31/-0.37	0.59/-0.71
Flack parameter	0	0.03(2)	0

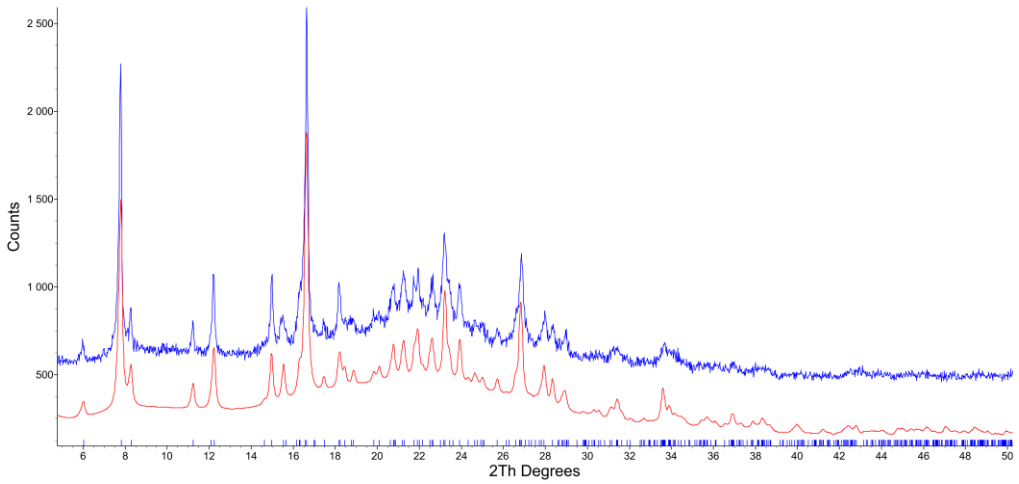

Fig. S1. Theoretical (red line) and experimental (blue line) powder patterns of compound **1**

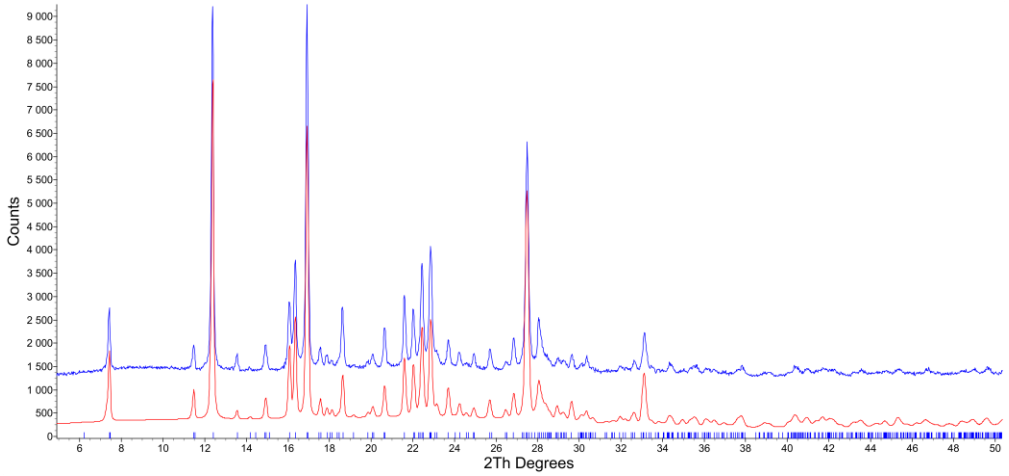

Fig. S2. Theoretical (red line) and experimental (blue line) powder patterns of compound **2**.

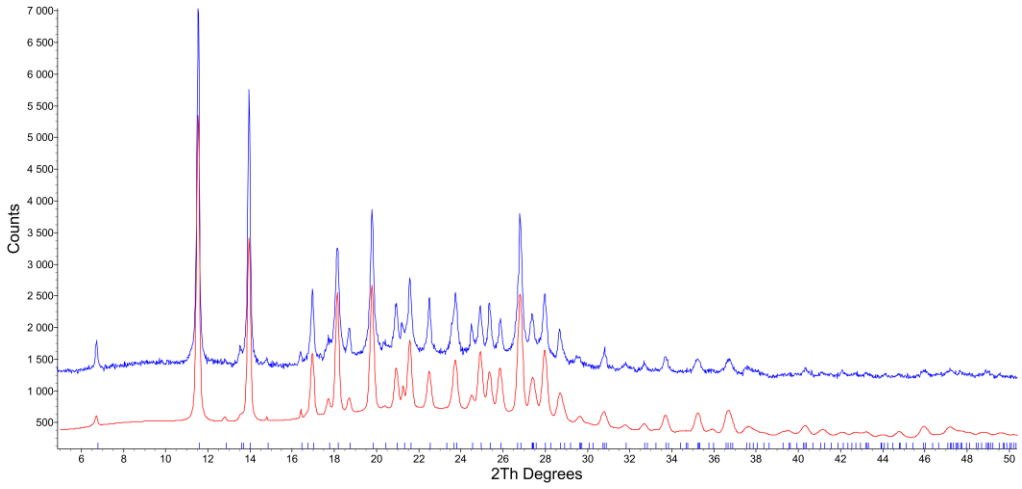

Fig. S3. Theoretical (red line) and experimental (blue line) powder patterns of compound **3**.

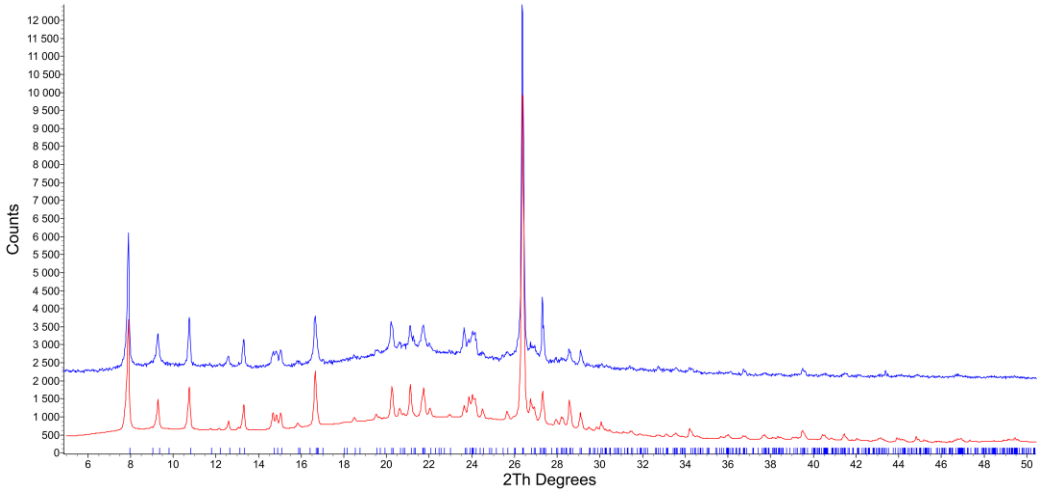

Fig. S4. Theoretical (red line) and experimental (blue line) powder patterns of compound **4**.

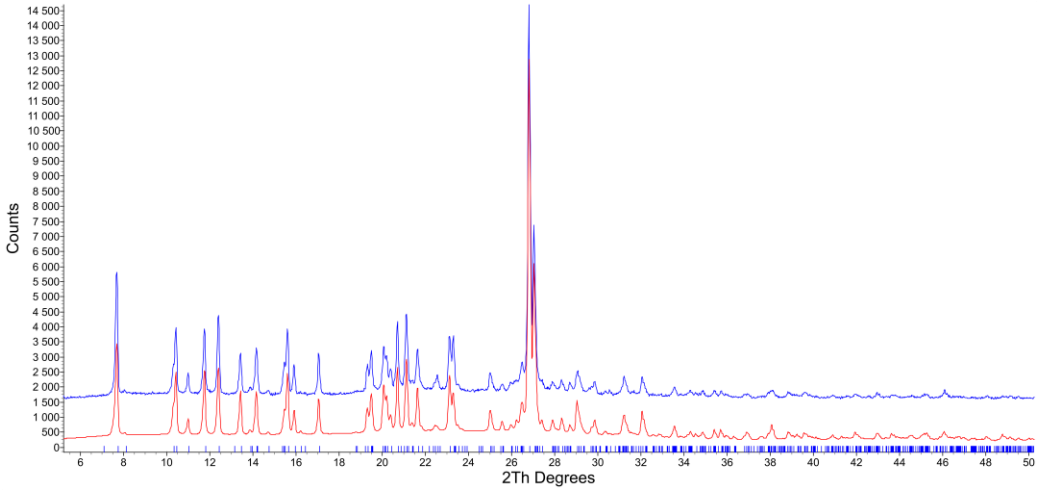

Fig. S5. Theoretical (red line) and experimental (blue line) powder patterns of compound **5**.

Table S2. Intermolecular hydrogen bonds in compounds **1-5**.

	D-H…X	d(H…X)	d(D…X)	(DHX)		D-H…X	d(H…X)	d(D…X)	(DHX)
1	*-1+x, y, z (intrachain)*				**4**	*1/2-x,y,1/2+z*			
	C10-H10…Cl2	2.5790(12)	3.455(5)	157.1(3)		O1-H1…N6	2.046(4)	2.823(5)	158.0(3)
	1-x, 2-y, 1-z					x,1/2-y,1/2+z			
	C3-H3…Cl2	2.8160(11)	3.661(5)	151.6(3)		C1-H1A…S1	2.7953(18)	3.367(6)	120.7(4)
	C2-H2A…Cl2	2.8876(11)	3.800(5)	166.7(3)		C11-H11…S1	3.173(2)	4.068(6)	162.0(3)
	C2-H2A…N2	2.567(4)	3.099(6)	116.7(3)		C12-H12…S1	2.8748(18)	3.764(6)	160.6(3)
	2-x, 1-y, 1-z					C18-H18…S1	3.0328(18)	3.899(6)	155.7(3)
	O1-H1…O1	2.566(4)	3.026(7)	116.8(2)		*-x,-y,1-z*			
	3/2-x,-1/2+y,3/2-z					C10-H10…S2	2.7729(16)	3.604(6)	149.6(4)
	C12-H12…Cl1	3.0767(12)	3.984(5)	165.3(3)		*1/2+x,-y,3/2-z*			
	C11-H11…Cl1	2.8931(12)	3.799(5)	165.1(3)		C16-H16…S2	3.0862(17)	3.908(8)	148.3(5)
2	*1-x, 1+y, 1-z (intrachain)*					*1-x,-y,1-z*			
	C1-H1A…Cl2	2.6186(11)	3.536(4)	162.5(3)		C8-H8…S2	3.0642(17)	3.960(6)	161.9(4)
	C3-H3…Cl2	2.8125(11)	3.735(4)	164.1(3)	**5**	1-x,2-y,1-z			
	C1'-H1'A…Cl1	2.8303(13)	3.714(5)	155.1(2)		C2'-H2'...N2'	2.435(3)	3.192(5)	136.4(3)
	C3'-H3'…Cl1	2.6681(11)	3.551(5)	154.9(3)		C11'-H11'…N2A	2.815(3)	3.466(5)	126.6(2)
	1+x,1+y,z					C11'-H11'…N1A	3.009(3)	3.548(6)	117.4(3)
	C2-H2…O1'	2.288(4)	3.228(7)	169.9(3)		*-x,-y,-z*			
	C2-H2…O2'	2.658(3)	3.116(6)	110.2(3)		C6-H6…S1A	2.9397(11)	3.777(4)	147.66(16)
	x,1+y,z					*-1+x,y,z*			
	C2'-H2'…O1	2.282(4)	3.218(7)	168.3(3)		C1'-H1'A…S1A	2.8325(13)	3.667(5)	147.22(19)
	C2'-H2'…O2	2.578(3)	3.138(5)	118.1(3)		*-1-x,-y,-z*			
3	*x, -1+y, z (intrachain)*					C10-H10…S1A	3.2001(11)	3.805(4)	123.2(3)
	C1-H1A-S1A	2.9148(14)	3.823(5)	158.3(3)		*-x,1-y,-z*			
	C3-H3…N1A	2.875(5)	3.734(7)	149.4(3)		C1-H1A…S2A	2.7626(11)	3.706(4)	171.9(2)
	3/2-x,1/2+y,1-z					C12-H12…S2A	2.9646(11)	3.870(4)	159.7(2)
	C2-H2…O1	2.346(4)	3.301(6)	173.0(3)		*1-x,1-y,-z*			
	C2-H2…O2	2.550(3)	3.171(6)	122.5(3)		C2-H2…S2A	3.1353(11)	3.959(4)	146.1(3)
	O1-H1…O2	2.55(6)	3.004(5)	123(5)					

Hirshfeld surface analysis

Table S3. 2D fingerprint plots, Hirshfeld contact surfaces and derived «random contacts» and «enrichment ratios» for **1** and **2**. The enrichment ratios were not computed when the "random contacts" were lower than 0.9%, as they are not meaningful. Data for Zn is not provided due to the low contact percentage (< 0.1%).

	1						**2**				
	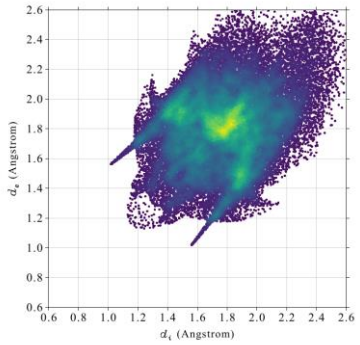						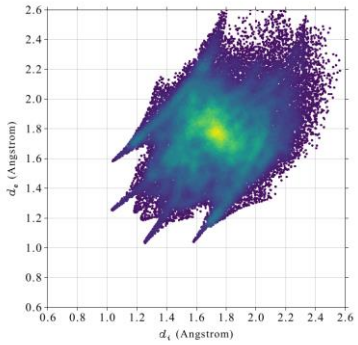				
Individual Contacts (Inner(row)/Outer(column), %)											
	H	C	N	O	Cl		H	C	N	O	Cl
H	24.7	7.5	5.7	3.8	9.8		23.3	5	7.5	6.8	8.9
C	9.2	2.1	2.6	0.6	1.3		7.4	2	2.8	0.5	1.9
N	6.5	2.5	1.6	0.5	0.8		8.5	2.7	0	0.2	0.1
O	4.2	0.4	0.4	0	0		7.6	0.4	0.2	0	0
Cl	13	1.2	0.8	0	0		11.3	1.8	0.1	0	0.1
Contacts (C(XX) or C(XY)+C(YX),%)											
H	24.7	16.8	12.2	7.9	22.8		23.3	12.4	16.1	14.4	20.2
C		2.1	5.2	0.9	2.5			2	5.5	0.9	3.7
N			1.6	0.9	1.6				0	0.5	0.2
O				0	0					0	0
Cl					0						0.1
Surfaces (S, %)											
	54.6	14.8	11.9	4.9	13.5		55.1	13.3	11.2	7.9	12.2
Random contacts (R, %)											
H	29.8	16.2	13	5.3	14.7		30.4	14.7	12.3	8.7	13.4
C	16.2	2.2	3.5	1.5	4			1.8	3	2.1	3.2
N	13	3.5	1.4	1.2	3.2				1.2	1.8	2.7
O	5.3	1.5	1.2	0.2	1.3					0.6	1.9
Cl	14.7	4	3.2	1.3	1.8						1.5
Enrichment ratios (E)											
	H	C	N	O	Cl		H	C	N	O	Cl
H	0.8	1	0.9	1.5	1.6		0.8	0.8	1.3	1.6	1.5
C		1	1.5	0.6	0.6			1.1	1.9	0.4	1.1
N			1.2	0.8	0.5				0	0.3	0.1
O				0	0					0	0
Cl					0						0.1

Table S4. 2D fingerprint plots, Hirshfeld contact surfaces and derived «random contacts» and «enrichment ratios» for **3-5**. The enrichment ratios were not computed when the "random contacts" were lower than 0.9%, as they are not meaningful. Data for Zn is not provided due to the low contact percentage (< 0.1%)

3							**4**						**5**				
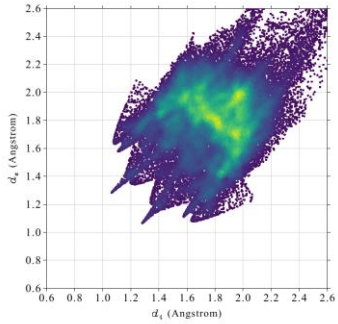							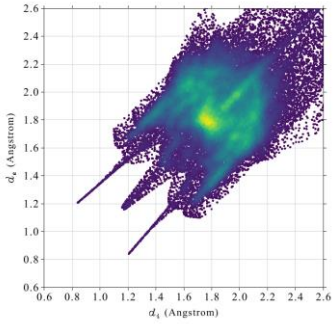						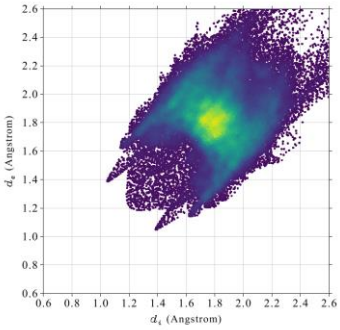				
Individual Contacts (Inner atom(row)/Outer atom(column), %)																	
	H	C	N	O	S		H	C	N	O	S		H	C	N	O	S
H	13.4	10.2	9.7	6.5	6.8		22	8.5	7.4	1.8	7.1		18.8	9.3	7.8	1.9	9
C	12.8	2.7	2.3	0.1	0.8		11	3.1	3.6	0.9	0.4		11.1	7.5	3.6	0.7	0.2
N	11.1	2.2	0.1	0.1	1.4		8.5	3.5	1.9	0.9	0.5		8.9	3.7	0	0.7	0.4
O	6.9	0	0.1	0	0		1.9	0.8	0.9	0.0	0.2		2.1	0.6	0.7	0	0.5
S	9.7	0.9	1.5	0	0.8		11.7	0.6	0.5	0.3	1.5		11.0	0.3	0.4	0.7	0
Contacts (C(XX) or C(XY)+C(YX),%)																	
H	13.4	23	20.8	13.4	16.6		22	19.5	16.0	3.7	18.9		18.8	20.4	16.6	4	20
C		2.7	4.4	0.1	1.6			3.1	7.1	1.7	1.0			7.5	7.3	1.3	0.5
N			0.1	0.2	2.9				1.9	1.8	0.9				0	1.4	0.8
O				0	0					0.0	0.5					0	1.2
S					0.8						1.5						0
Surfaces (S, %)																	
	50.3	17.2	14.2	6.9	11.3		51.1	17.9	14.8	3.9	12.1		49.4	22.3	13.1	4	11.3
Random contacts (R, %)																	
H	25.3	17.4	14.3	7	11.4		26.1	18.3	15.1	4	12.4		24.4	22	12.9	3.9	11.1
C		3.0	4.9	2.4	3.9			3.2	5.3	1.4	4.3		22	5	5.8	1.8	5
N			2.0	2	3.2				2.2	1.1	3.6		12.9	5.8	1.7	1	3
O				0.5	1.6					0.2	0.9		3.9	1.8	1	0.2	0.9
S					1.3						1.5		11.1	5	3	0.9	1.3
Enrichment ratios (E)																	
H	0.5	1.3	1.5	1.9	1.5		0.8	1.1	1.1	0.9	1.5		0.8	0.9	1.3	1	1.8
C		0.9	0.9	0.1	0.4			1.0	1.3	1.3	0.2			1.5	1.3	0.7	0.1
N			0	0.1	0.9				0.9	1.6	0.3				0	1.4	0.3
O				0	0					0.0	0.5					0	0
S					0.6						1.0						0

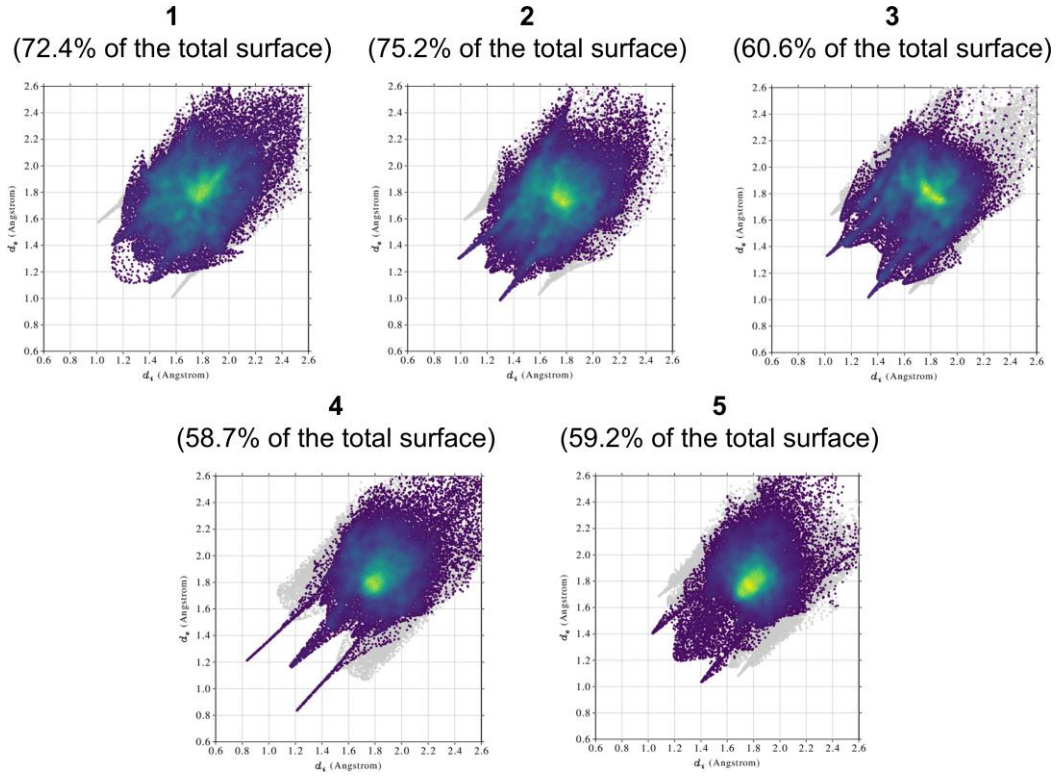

Fig. S6. 2D fingerprint plots for ligands' Hirshfeld surfaces part of complexes **1-5**. *Note:* since Multiwfn3.8 has a low-capacity character buffer for reading atomic indices in Hirshfeld surface analysis subroutine (2000 chars only), it was recompiled with a higher capacity buffer, accommodating 10000 chars.

QTAIM analysis of electron density from periodic quantum-chemical calculations.

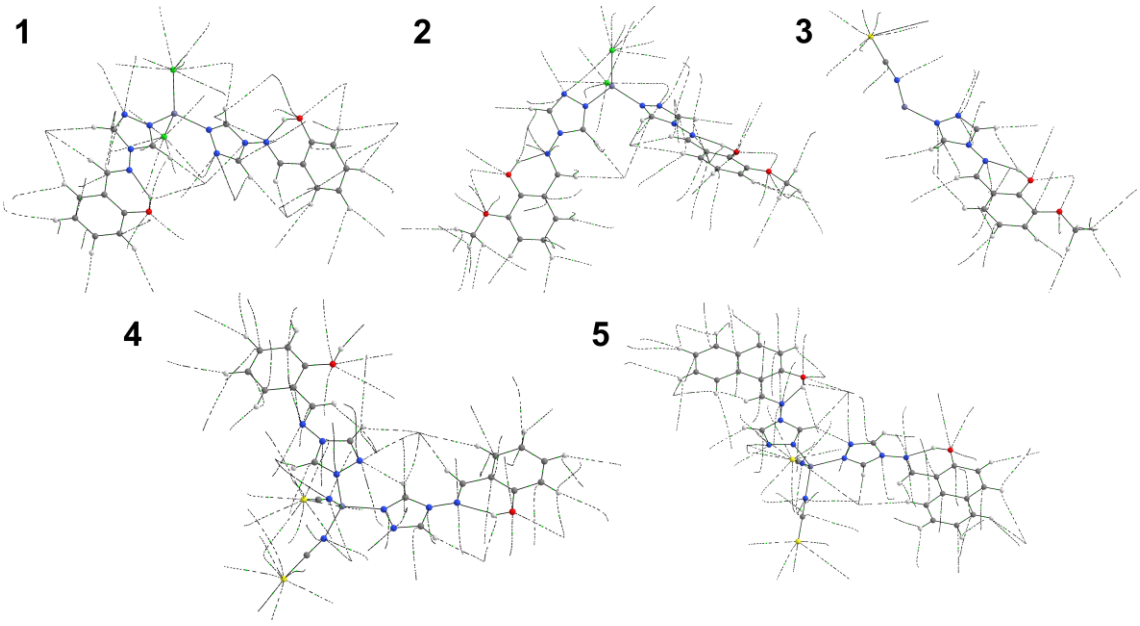

Fig. S7. All the located BCPs (green dots) and bond paths for compounds **1-5**. Intermolecular bond paths are indicated by dashed lines; intramolecular bonds are shown with solid lines.

Calculated electronic transitions

Table S5. Results of the TD-DFT functional prescreening: vertical excitation energies (λ, nm) and oscillator strengths (fosc) for the 20 lowest excited states of compounds **1-5**. Calculations employed a polarizable continuum solvation model (water) as a proxy for the crystal lattice.

PBE0		**TPSSh**		**CAM**		**WB97X-D4rev**	
λ (nm)	fosc	λ (nm)	fosc	λ (nm)	fosc	λ (nm)	fosc
1							
323.0	0.1904	349.7	0.0047	299.5	0.2660	290.3	0.3065
319.9	0.2039	345.6	0.1295	296.7	0.3177	287.6	0.3858
287.0	0.0000	344.9	0.0184	258.7	0.5059	251.9	0.4472
284.4	0.0001	342.2	0.1301	256.1	0.6140	249.9	0.5172
272.9	0.5861	294.2	0.0025	222.5	0.0031	218.4	0.0024
269.5	0.7716	293.6	0.0019	220.1	0.0011	216.2	0.0011
249.4	0.0002	287.4	0.0287	209.6	0.4383	205.7	0.6217
248.8	0.0002	285.9	0.0086	208.8	0.4363	204.5	0.6106
244.2	0.0045	285.1	0.5215	207.4	0.0009	193.5	0.0876
242.4	0.0005	281.5	0.6272	207.4	0.0007	193.0	0.0912
238.5	0.0003	279.9	0.0791	196.8	0.0462	185.5	0.0350
237.6	0.0009	277.9	0.1488	196.7	0.1501	183.8	0.0248
234.9	0.0006	276.3	0.0049	194.9	0.0803	180.8	0.0831
233.4	0.0005	274.6	0.0065	192.8	0.0315	180.7	0.0689
233.0	0.0031	270.4	0.0015	188.3	0.0031	178.5	0.0033
231.2	0.0007	269.1	0.0028	187.7	0.0007	177.6	0.0027
229.4	0.0002	251.0	0.0030	187.4	0.0009	173.0	0.2975
228.5	0.0000	250.5	0.0049	186.9	0.0002	172.4	0.2535
222.3	0.0092	248.5	0.0022	185.8	0.0171	171.6	0.0608
2							
368.6	0.0631	409.3	0.0382	326.7	0.1237	310.6	0.1776
358.0	0.0567	406.0	0.0023	319.4	0.1044	304.6	0.1435
323.6	0.0000	396.1	0.0282	276.1	0.5084	267.8	0.4437
315.6	0.0000	394.5	0.0093	273.0	0.9455	265.2	0.9237
293.7	0.5867	323.3	0.0006	226.9	0.0009	223.3	0.0008
289.4	0.9125	322.9	0.0004	225.3	0.0000	216.5	0.0030
271.1	0.0004	309.0	0.5840	221.0	0.0000	214.2	0.5774
270.9	0.0004	303.8	0.8254	219.9	0.0023	208.7	0.6295
247.9	0.0001	292.2	0.0004	216.0	0.5387	199.3	0.0465
246.7	0.0001	291.1	0.0001	210.7	0.5920	197.9	0.0636
244.3	0.0017	282.5	0.0003	208.8	0.0073	193.0	0.0311
240.5	0.0018	281.4	0.0009	206.4	0.0051	189.9	0.0319
239.9	0.0009	278.7	0.0006	201.7	0.0018	188.3	0.0521
238.1	0.0005	277.1	0.0002	201.6	0.0017	186.9	0.0229
235.0	0.0002	276.2	0.0000	200.6	0.0259	182.3	0.0223

234.4	0.0001	275.4	0.0003	199.1	0.0339	181.4	0.0159
233.2	0.0196	260.8	0.0114	195.1	0.0140	181.0	0.3655
230.7	0.0002	254.7	0.0001	193.1	0.0044	180.1	0.0119
228.1	0.0108	254.4	0.0043	192.3	0.0003	179.7	0.0618
3							
358.0	0.1209	396.0	0.0510	320.4	0.2210	306.4	0.2929
357.8	0.0087	395.9	0.0013	319.9	0.0474	305.7	0.1015
315.5	0.0000	394.0	0.0281	279.1	0.4444	270.7	0.3819
315.5	0.0000	394.0	0.0008	276.3	1.0742	268.4	1.0162
310.4	0.0006	377.6	0.0004	224.7	0.0013	225.2	0.0000
308.8	0.0000	375.8	0.0000	224.1	0.0000	224.6	0.0001
304.4	0.0161	369.0	0.0027	223.6	0.0016	218.8	0.0007
302.9	0.0133	367.3	0.0006	222.9	0.0023	218.8	0.0056
300.6	0.0082	363.4	0.0007	222.4	0.0000	215.5	0.0034
299.0	0.0046	361.7	0.0005	222.4	0.0005	215.4	0.0000
295.8	0.4903	350.7	0.0032	220.9	0.0002	214.2	0.0000
292.6	0.7344	349.1	0.0011	220.9	0.0000	213.4	0.0006
291.0	0.3208	326.9	0.0013	220.2	0.0053	206.2	0.4618
290.0	0.0058	326.8	0.0006	218.9	0.0006	205.6	0.7740
273.8	0.0010	310.0	0.5156	218.6	0.0018	195.9	0.0549
273.8	0.0005	305.9	0.9860	216.5	0.0022	195.9	0.0704
233.5	0.0004	253.6	0.0181	215.7	0.0002	189.9	0.0261
233.4	0.0049	253.6	0.0037	214.2	0.0040	189.6	0.0242
227.0	0.0253	249.5	0.0015	214.0	0.0032	187.3	0.0091
4							
319.8	0.3297	357.9	0.0003	297.1	0.4253	288.1	0.4675
318.2	0.2170	356.2	0.0001	293.9	0.3118	284.3	0.3629
295.3	0.0005	352.8	0.0048	252.6	0.4012	245.7	0.3396
293.7	0.0001	351.1	0.0006	248.6	0.5007	242.5	0.4190
291.8	0.0030	347.5	0.0003	223.2	0.0015	220.5	0.0000
290.1	0.0003	346.4	0.0000	218.5	0.0000	219.6	0.0015
287.6	0.0002	342.9	0.0896	217.8	0.0002	219.5	0.0000
286.9	0.0000	342.7	0.0151	216.8	0.0017	213.3	0.0019
282.3	0.0010	342.0	0.1449	215.0	0.0020	212.0	0.0013
281.4	0.0002	340.9	0.1566	213.3	0.0061	211.8	0.0004
281.2	0.0000	339.8	0.0028	213.1	0.0017	210.7	0.0003
280.9	0.0001	338.5	0.0003	212.4	0.0018	210.6	0.0009
267.2	0.5284	287.3	0.0013	211.7	0.0022	205.1	0.6641
262.2	0.6179	280.7	0.0028	211.3	0.0017	202.2	0.3475
242.9	0.0000	279.2	0.5956	210.2	0.0026	191.5	0.3454
238.4	0.0001	274.0	0.6525	210.1	0.0070	190.6	0.0443
236.3	0.0013	249.4	0.0011	209.4	0.0049	189.1	0.1157
227.7	0.0010	244.9	0.0004	209.1	0.2450	186.9	0.0008

223.0	0.0098	243.4	0.0104	208.9	0.2052	186.1	0.0025
5							
361.3	0.6102	394.7	0.0000	335.3	0.7277	324.5	0.7650
356.7	0.2640	391.0	0.0004	332.0	0.2704	321.6	0.2745
320.9	0.0000	383.5	0.4966	292.2	0.2001	281.9	0.2380
318.2	0.0000	378.0	0.2493	290.0	0.1475	279.5	0.1652
317.8	0.1174	376.6	0.0010	256.7	0.0169	249.5	0.0209
316.4	0.0924	376.4	0.0069	255.4	0.0245	248.6	0.0382
311.4	0.0010	371.7	0.0027	235.4	0.1471	227.6	0.3789
311.1	0.0000	371.3	0.0073	234.7	0.1435	227.3	0.0000
306.6	0.0003	369.6	0.0003	227.6	0.0191	227.0	0.3322
306.3	0.0006	368.7	0.0001	226.7	0.0140	224.1	0.0001
305.9	0.0003	363.4	0.0001	226.4	0.0011	222.3	0.0012
305.6	0.0003	362.9	0.0002	226.3	0.0423	221.7	0.0059
299.1	0.0002	341.3	0.0787	225.0	0.0427	218.0	0.0005
299.0	0.0004	340.8	0.0617	224.8	0.0093	218.0	0.0002
278.4	0.0000	336.3	0.0001	223.9	0.3877	215.3	0.0012
273.5	0.0076	329.7	0.0000	223.7	0.0008	215.3	0.0005
273.4	0.0002	288.3	0.0027	223.4	0.0938	209.1	0.4399
271.0	0.0080	285.3	0.0017	223.1	0.0045	208.5	0.2235
252.9	0.2377	282.9	0.0002	222.0	0.0165	205.8	0.9599

Table S6. Results of the TD-DFT functional prescreening: vertical excitation energies (λ, nm) and oscillator strengths (fosc) for the 20 lowest excited states of compounds **1-5**. Calculations employed a QM1/QM2 approach to account for crystal lattice.

PBE0		**TPSSh**		**CAM-B3LYP**		**WB97X-D4rev**	
λ (nm)	fosc	λ (nm)	fosc	λ (nm)	fosc	λ (nm)	fosc
1							
443.4	0.0002	608.8	0.0001	318.2	0.2293	307.7	0.2671
432.2	0.0002	591.7	0.0003	313.4	0.2608	303.3	0.3202
428.6	0.0062	581.7	0.0050	291.2	0.0008	257.9	0.4158
419.1	0.0021	567.5	0.0014	284.1	0.0036	254.9	0.4326
404.5	0.0002	541.1	0.0001	283.4	0.0089	235.1	0.0006
395.7	0.0020	527.4	0.0014	277.8	0.0070	229.7	0.0020
391.7	0.0009	516.8	0.0004	274.1	0.0007	227.6	0.0000
381.5	0.0013	503.4	0.0008	268.9	0.0104	225.9	0.0017
343.1	0.1524	404.9	0.0002	267.5	0.0687	225.3	0.0002
337.9	0.1708	396.0	0.0217	264.6	0.3861	223.2	0.0008
325.8	0.0001	376.3	0.0003	261.4	0.4541	221.6	0.0017
319.2	0.0116	371.3	0.0035	259.3	0.0510	218.3	0.0029
308.8	0.0001	366.5	0.1132	237.8	0.0002	216.8	0.0010

304.1	0.0000	359.6	0.1017	235.1	0.0028	210.3	0.0564
292.2	0.0388	355.2	0.0029	234.9	0.0018	209.1	0.3527
286.3	0.0026	349.3	0.0003	233.0	0.0008	208.4	0.4064
278.7	0.5056	309.9	0.0002	222.6	0.0000	202.9	0.0987
273.5	0.6274	309.2	0.0007	219.1	0.0011	200.2	0.0269
261.7	0.0007	308.1	0.0001	218.8	0.0053	198.4	0.0106
258.5	0.0017	304.5	0.0010	214.4	0.2547	197.5	0.0735
2							
462.0	0.0002	635.7	0.0002	345.0	0.1578	327.0	0.2187
450.2	0.0000	612.2	0.0000	343.4	0.0585	325.1	0.0890
446.3	0.0007	608.7	0.0003	302.8	0.0003	273.7	0.3662
435.6	0.0070	586.2	0.0051	297.8	0.0004	269.4	0.7700
426.1	0.0003	570.3	0.0006	295.1	0.0159	242.4	0.0002
416.8	0.0031	552.8	0.0019	291.6	0.0404	240.5	0.0007
412.3	0.0009	548.0	0.0005	289.2	0.0002	237.8	0.0013
402.9	0.0004	532.0	0.0002	283.1	0.1298	236.9	0.0013
388.5	0.0779	445.4	0.0010	282.3	0.2528	234.9	0.0005
387.2	0.0309	429.1	0.0712	280.4	0.0761	230.9	0.0013
352.1	0.0005	428.3	0.0100	276.9	0.7192	227.3	0.0013
342.0	0.0189	424.1	0.0037	274.0	0.0058	223.6	0.0009
335.8	0.0162	419.5	0.0020	249.5	0.0004	222.1	0.0004
333.2	0.0524	410.9	0.0308	243.9	0.0049	220.6	0.0012
299.4	0.3889	356.2	0.0219	241.4	0.0004	215.0	0.4226
294.8	0.3428	348.7	0.0086	234.3	0.0014	213.6	0.6219
290.3	0.3880	341.4	0.0008	233.7	0.0009	210.7	0.0212
288.7	0.0666	328.0	0.0016	233.4	0.0002	207.0	0.0148
285.4	0.0090	313.7	0.0093	218.6	0.0283	204.8	0.0055
276.0	0.0015	311.5	0.4430	217.6	0.3143	204.6	0.0067
3							
816.9	0.0008	1458.0	0.0009	417.2	0.0010	329.9	0.2126
796.7	0.0001	1413.2	0.0001	410.1	0.0032	328.7	0.0803
792.0	0.0028	1384.0	0.0031	408.4	0.0001	303.8	0.0017
772.8	0.0008	1341.4	0.0010	402.6	0.0009	299.8	0.0063
752.8	0.0003	1270.8	0.0004	397.7	0.0004	297.5	0.0000
735.1	0.0001	1232.9	0.0002	391.2	0.0007	295.4	0.0005
724.5	0.0041	1193.8	0.0053	389.1	0.0046	291.6	0.0015
708.5	0.0015	1163.1	0.0020	382.0	0.0021	288.5	0.0064
397.1	0.0845	450.9	0.0009	349.4	0.1556	286.7	0.0096
396.5	0.0138	445.4	0.0118	348.5	0.0421	282.2	0.0095
360.0	0.0010	445.2	0.0041	282.6	0.3811	273.5	0.3221
355.2	0.0011	443.7	0.0007	278.0	0.9243	269.6	0.8699
351.4	0.0001	439.6	0.0430	256.2	0.0016	241.2	0.0000
351.3	0.0001	439.3	0.0049	253.8	0.0002	239.9	0.0001

347.3	0.0003	431.2	0.0003	250.1	0.0004	230.7	0.0024
344.8	0.0000	430.4	0.0000	248.5	0.0000	230.4	0.0000
341.1	0.0021	423.6	0.0004	246.2	0.0006	228.7	0.0009
340.2	0.0005	422.3	0.0014	245.9	0.0010	228.4	0.0008
333.0	0.0024	412.1	0.0013	242.6	0.0016	224.7	0.0008
327.4	0.0010	404.3	0.0005	242.2	0.0001	224.6	0.0071
4							
722.9	0.0000	1236.2	0.0000	381.1	0.0000	304.4	0.3852
702.5	0.0000	1181.5	0.0000	373.9	0.0000	293.4	0.4613
661.6	0.0001	1058.4	0.0000	364.8	0.0002	280.9	0.0000
656.2	0.0003	1049.1	0.0003	362.9	0.0006	276.4	0.0003
646.5	0.0039	1016.9	0.0045	360.6	0.0061	273.0	0.0003
630.7	0.0001	991.0	0.0002	352.8	0.0002	271.4	0.0012
597.5	0.0002	911.0	0.0002	341.5	0.0006	270.6	0.0065
579.3	0.0001	869.8	0.0001	335.2	0.0004	264.5	0.0002
341.2	0.0001	432.4	0.0000	313.8	0.3240	258.5	0.0205
337.3	0.2219	425.6	0.0003	301.6	0.4068	258.0	0.2818
336.6	0.0008	408.9	0.0001	265.5	0.3642	255.2	0.3602
330.8	0.0004	407.0	0.0002	261.9	0.4879	254.4	0.0340
326.9	0.0015	403.0	0.0003	247.0	0.0002	241.5	0.0000
325.7	0.0036	399.8	0.0003	243.8	0.0005	239.9	0.0000
322.8	0.2794	397.9	0.0002	240.5	0.0012	232.3	0.0121
320.5	0.0002	394.0	0.0012	239.6	0.0001	230.7	0.0007
319.2	0.0000	391.9	0.0000	237.8	0.0009	230.5	0.0004
316.8	0.0009	389.8	0.0000	237.5	0.0118	228.1	0.0003
315.7	0.0005	386.3	0.0003	237.0	0.0007	227.8	0.0002
315.5	0.0000	385.6	0.0003	234.7	0.0014	223.1	0.0008
5							
672.9	0.0012	1056.3	0.0013	375.8	0.0039	340.5	0.6109
663.7	0.0000	1033.1	0.0000	373.1	0.0000	333.2	0.3217
617.0	0.0001	941.9	0.0002	357.8	0.0005	287.5	0.1983
616.1	0.0003	930.6	0.0001	356.8	0.0139	284.0	0.1629
610.1	0.0004	920.5	0.0030	352.2	0.5532	282.6	0.0012
607.7	0.0028	910.5	0.0006	349.7	0.0118	281.2	0.0002
563.2	0.0002	835.0	0.0002	347.8	0.0366	273.1	0.0005
556.1	0.0004	817.9	0.0004	342.8	0.2629	272.4	0.0005
380.9	0.3622	489.6	0.0004	328.9	0.0002	264.0	0.0004
379.6	0.0906	484.3	0.0000	326.5	0.0001	262.6	0.0013
376.8	0.0001	474.2	0.0000	301.0	0.1490	257.0	0.0155
368.7	0.2871	469.0	0.0004	295.3	0.1491	256.1	0.0113
366.4	0.0014	461.0	0.0001	264.6	0.0313	250.6	0.0005
363.4	0.0019	456.0	0.0003	263.7	0.0166	249.0	0.0003
362.0	0.0002	445.7	0.0000	257.0	0.0007	239.4	0.0000

359.6	0.0001	440.8	0.0001	255.9	0.0001	237.9	0.0000
348.8	0.0002	433.6	0.0000	249.2	0.0007	231.7	0.1495
347.4	0.0000	408.8	0.0055	248.7	0.0003	230.7	0.0910
344.7	0.0000	404.2	0.3691	244.7	0.0000	230.2	0.1051
334.0	0.0727	389.7	0.2621	243.5	0.0008	228.3	0.0008

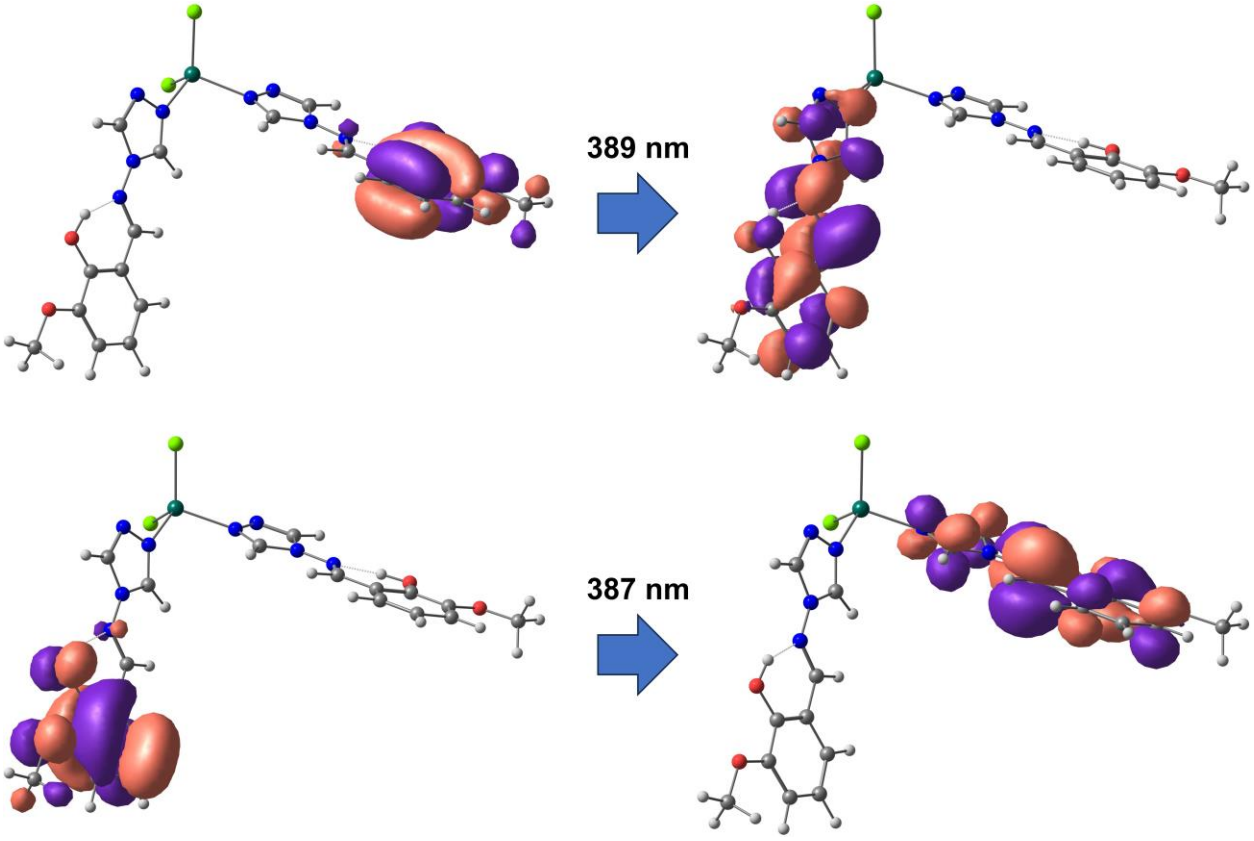

Fig. S8. Isosurface plots (contour value = 0.03 a.u.) of the dominant natural transition orbitals pairs (the weight for each transition exceeds 0.92) for **2**, corresponding to excitations with the highest oscillator strengths and closest to the experimental excitation wavelength.

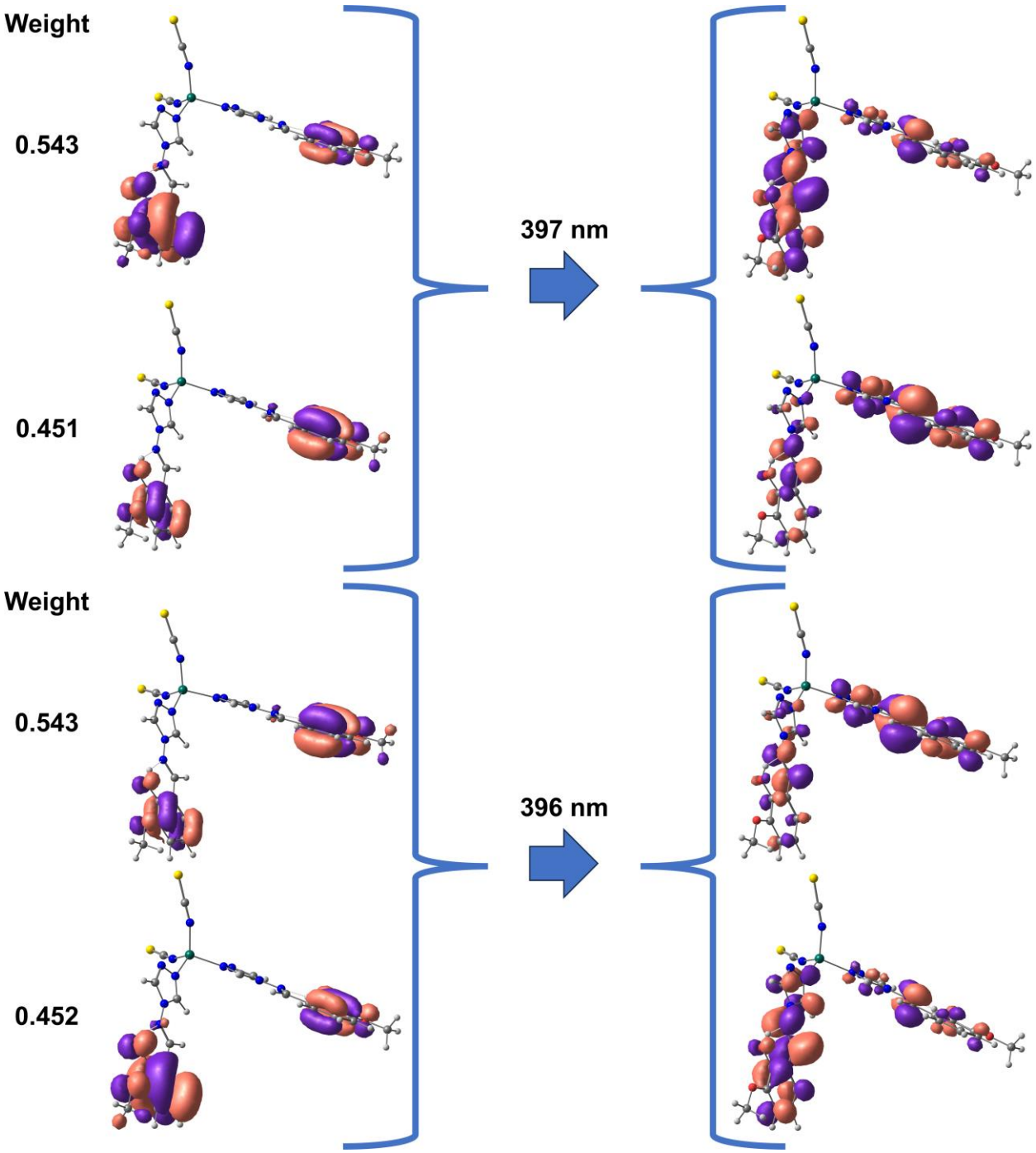

Fig. S9. Isosurface plots (contour value = 0.03 a.u.) of the dominant natural transition orbitals pairs for **3**, corresponding to excitations with the highest oscillator strengths and closest to the experimental excitation wavelength.

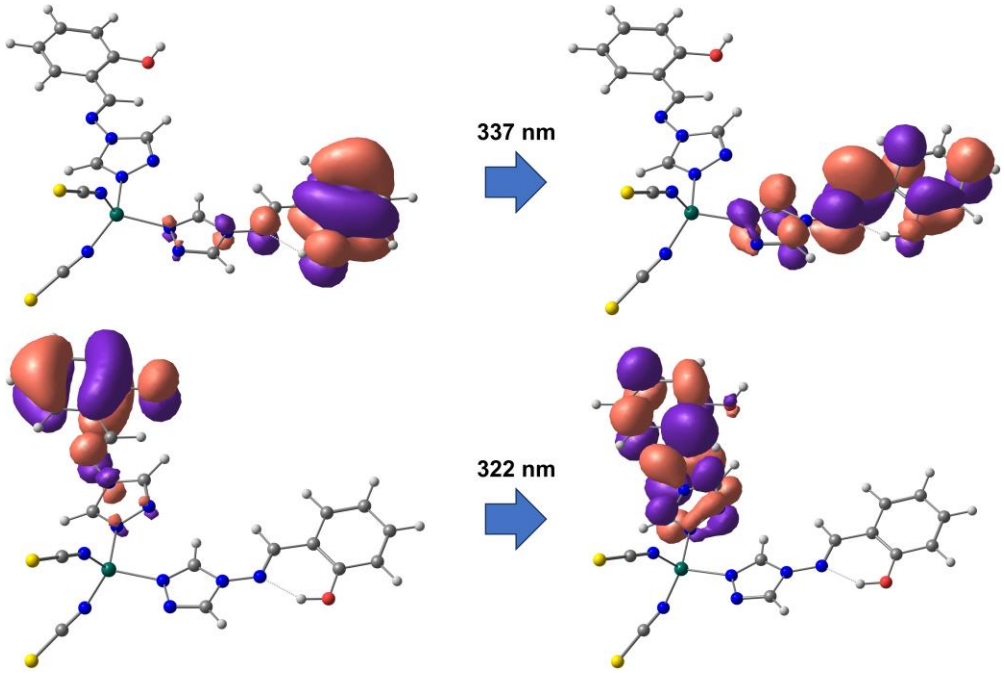

Fig. S10. Isosurface plots (contour value = 0.03 a.u.) of the dominant natural transition orbitals pairs (the weight for each transition exceeds 0.95) for **4**, corresponding to excitations with the highest oscillator strengths and closest to the experimental excitation wavelength.

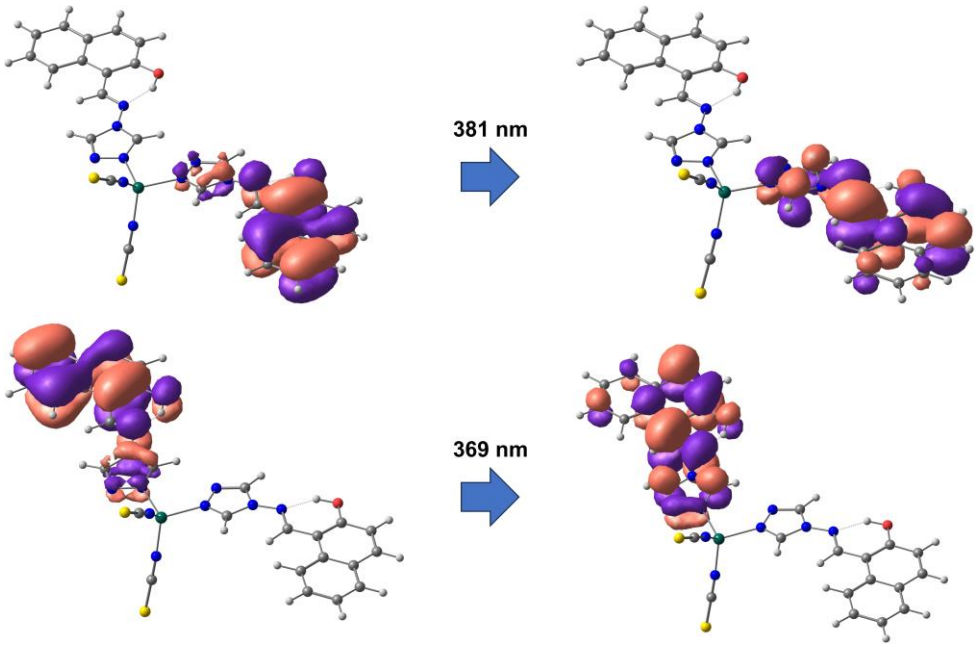

Fig. S11. Isosurface plots (contour value = 0.03 a.u.) of the dominant natural transition orbitals pairs (the weight for each transition exceeds 0.93) for **5**, corresponding to excitations with the highest oscillator strengths and closest to the experimental excitation wavelength.

Preliminary investigations on the proton transfer mechanism in compounds 1 and 5.

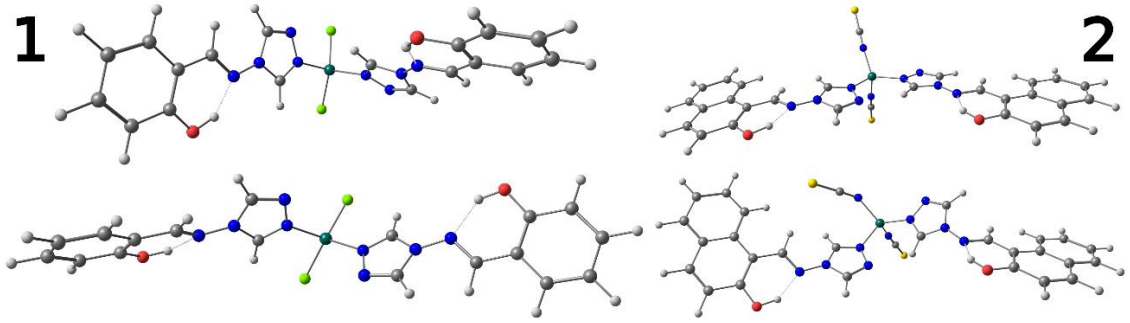

Fig. S12. Comparison of experimental and computed structures for complexes **1** and **5**. (Top) Geometries from X-ray crystallography. (Bottom) Fully optimized geometries of isolated molecules at PBE0-D4/def2-tzvp level of theory, computed with a polarizable continuum solvation model (water) as a proxy for the crystal field. The comparison clearly shows that a full gas-phase optimization leads to substantial structural deviations from the crystallographic geometries.

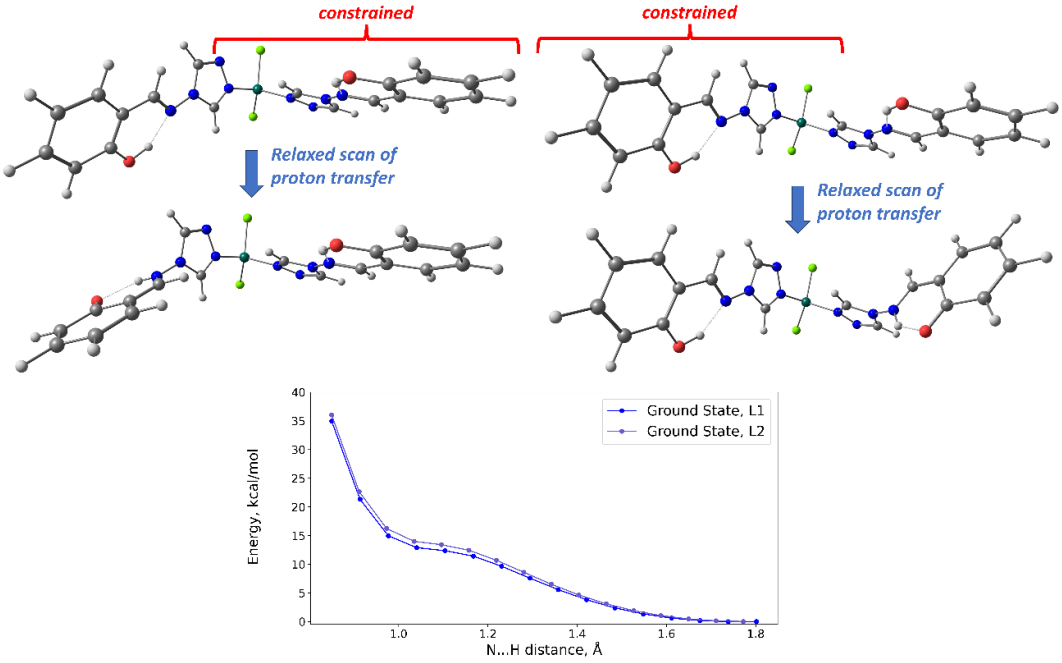

Fig. S13. Top: representative geometries from the relaxed potential energy surface (PES) scan for the ground state (S_0). The scan was performed for isolated molecule with constraints applied to the second ligand, the $ZnCl_2$ fragment, and the triazole ring of the first ligand at PBE0-D4/def2-tzvp level of theory. Despite the significant rotation of the imine and phenolic rings observed in the final geometry – a motion that is sterically hindered and unlikely to occur in the crystal lattice, no second minimum corresponding to the cis-keto form was located on the ground-state PES for both ligands (graphic below).

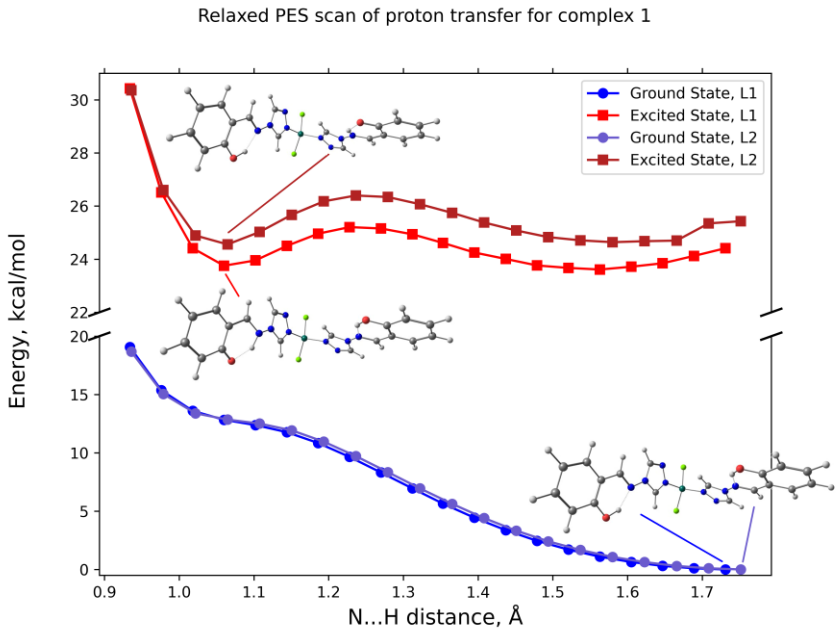

Fig. S14. Potential energy curves (PECs) of the ground (S_0) and excited ($S_{\pi\pi^*}$) states of the coordinated ligands in complex **1**. The PECs were obtained by scanning the proton transfer coordinate at the QM1/QM2 (PBE0/def2-TZVP & xTB2) level of theory. While the ground-state (S_0) PES shows no stable minimum for the keto form, the PES for the intraligand $\pi \rightarrow \pi^*$ excited state exhibits two distinct minima corresponding to the enol and cis-keto forms.

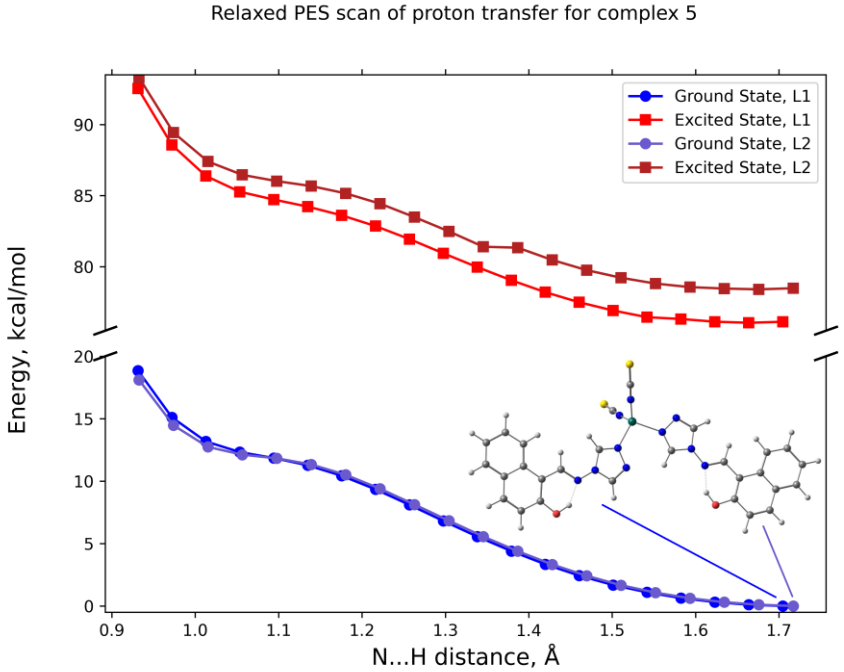

Fig. S15. Potential energy curves (PECs) of the ground (S_0) and excited ($S_{\pi\pi^*}$) states of the coordinated ligands in complex **5**. The PECs were obtained by scanning the proton transfer coordinate at the QM1/QM2 (PBE0/def2-TZVP & xTB2) level of theory. The potential energy surfaces for both the ground (S_0) and excited ($S_{\pi\pi^*}$) states show no stable minimum for the keto form.

Preliminary investigations on the photoreaction mechanism of isolated HL^3.

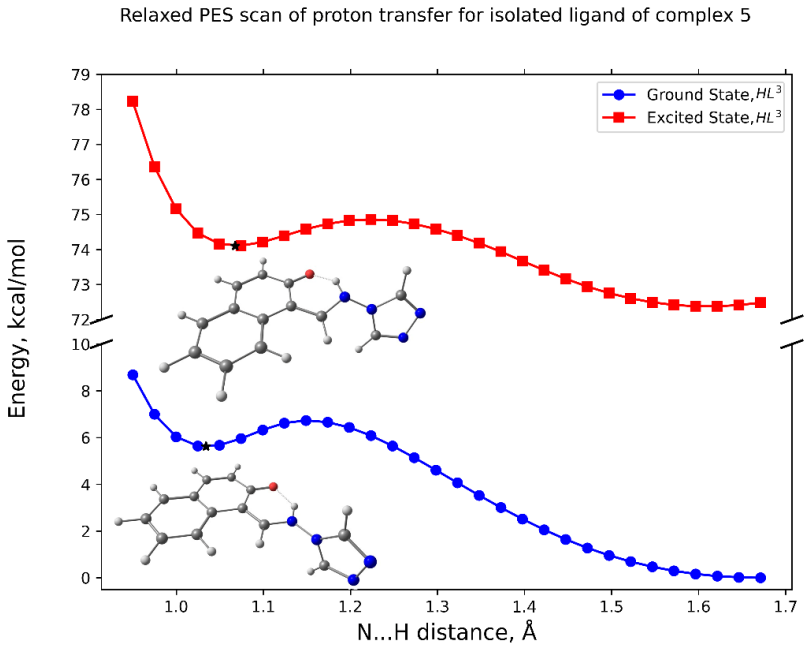

Fig. S16. Potential energy curves (PECs) of the ground (S_0) and excited ($S_{\pi\pi^*}$) states for HL^3 scanned along the proton transfer coordinate at the PBE0-D4/def2-TZVP level of theory.

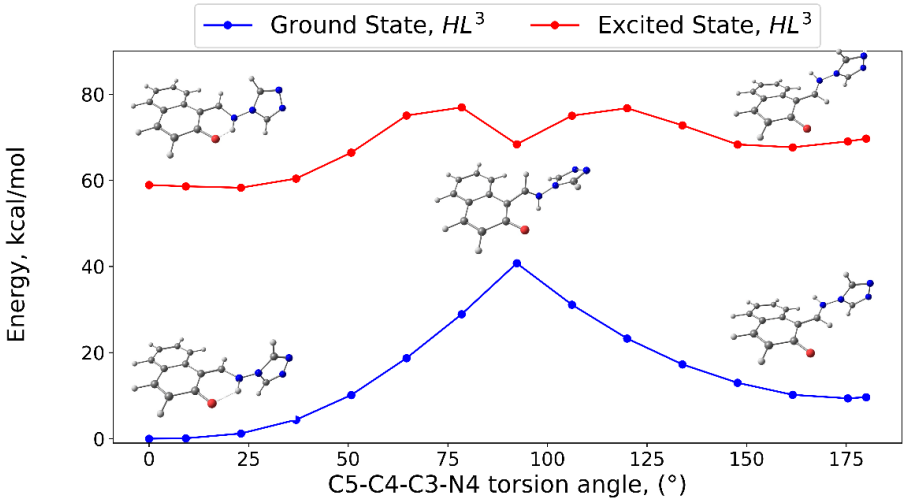

Fig. S17. Potential energy curves (PECs) for the ground (S_0) and excited ($S_{\pi\pi^*}$) states of HL^3. The PECs were computed by scanning the C5-C4-C3-N4 torsion angle. Single-point energy calculations were performed at the CASPT2(2,2)/def2-TZVP level on geometries pre-optimized at the PBE0-D4/def2-TZVP level. The presence of a local minimum on the $S_{\pi\pi^*}$ curve and a local maximum on the S_0 curve at a torsion angle of ~ 92° indicates a likely conical intersection, analogous to those reported for salicylidene-anilines [see J. M. Ortiz-Sánchez, R. Gelabert, M. Moreno and J. M. Lluch, J. Chem. Phys., 2008, 129, 214308 (*https://doi.org/10.1063/1.3032215*)].